NATO: Development of Biosensors using Carbon Nanotubes

S. Bellucci (Project Director), R. Baldini (Tecn.), S.Bistarelli (Dott.), M. Mastrucci (Bors. Tecn.), A. Cataldo (Dott..), F. Micciulla (Ass. Ric.)
External collaborating Institutions:
- Yerevan State Univ., Armenia

We direct the project Development of Biosensors using Carbon Nanotubes within the NATO Emerging Security Challenges Division, Science for Peace and Security Programme. The project has a duration of 42 months and started its activities on 1st October 2013. The consortium binds together a University and a Research Organization.

Introduction

Background

Biosensors are nowadays technological hot topics due to the possible applications in social interest fields such as defense and security, medical research and clinical diagnostic, health care, monitoring of environmental pollutants and in the food industry, scientific investigation, medicine, agriculture, chemical manufacturing, environment protection. Application of biosensors became one of widespread methods in antiterrorist defense.

Two strategies are applied to detect pollutants by biosensors:

The first one is the hybridization detection of nucleic acid sequences from infectious microorganisms. The proliferation of nucleic acid and immuno-based technologies has provided sensitive and specific detection systems for pathogenic bacteria and viruses. From a military point of view, there are a number of pathogenic bacteria which can be considered possible biological warfare agents. These microorganisms are resistant to environmental conditions, most of the human population is completely susceptible, and the diseases they cause are severe with a high fatality rate. A large number of these fatal organisms could easily be grown and preserved for several years. DNA detection is more specific than immunologically based detection, and the sensitivity can improve thanks to its combination with polymerase chain reaction (PCR) methods. Gene probes are already finding application in detection of disease-causing microorganisms in water supplies, food, or in plants, animal or human tissues.

The second strategy is the monitoring of pollutants interacting with the immobilized DNA layer (drugs, mutagenic pollutants, etc.), because the main aim of terrorists is the propagation of poisons, that express biological activity and in many cases are DNA damaging agents.

Besides the signal generated by the sensing device, the biosensor is constituted by the molecular recognition element and the transducer material. In spite of traditional analytic devices, bio-sensors have high selectivity and sensitivity. Such a high selectivity provides by biological transducers using the principle of specific binding (recognition) of substrate from environment. The molecular recognition element can be a biological molecule, such as DNA (deoxyribonucleic acid) single strand, proteins, enzymes, or a biological system, such as membrane, cell, etc.

At the present time optical, electrochemical and gravimetric methods of registration of DNA hybridization event are used. Optical DNA detection methods include the use of various intercalating dyes or rely on spectral interference of reflected white light. Amperometric or electrochemical biosensors use a variety of electrode types functionalized with DNA to monitor enzymatic reactions occurring upon hybridization of the desired target. Some electrical biosensors are based on monitoring the intrinsic molecular charge of DNA on field-effect sensors or upon hybridization of a target molecule on PNA probes immobilized on silicon nanowires. Other detection technologies utilize functionalized gold or platinum nanoparticles to detect hybridization events optically or electrically following silver enhancement. Various types of biosensors, including surface plasmon resonance and quartz crystal microbalance piezoelectric sensors can be applied for the detection of DNA fragments specific to genetically modified food compounds. The present Project is focused on the electrochemical DNA – sensors development.

Objectives

The main direction of the antiterrorist is the prevention and/or the early exposure of terroristic attacks. In case of using the biological warfare such as living agents or toxins DNA – biosensors yield one of the most effective tools for early diagnostics. The main objectives of the project are:

I) To create a prototype of one of the technologically state-of-the-art and most effective electrochemical DNA – biosensors.

ii) To investigate and to compare thermodynamics and kinetics of DNA and RNA hybridization both in the bulk and when immobilized on the surface of a substrate, e.g. an electrode

iii) To synthesize polymer – CNT nanocomposites as suitable candidates for biosensor electrodes.

iv) To investigate sensitivity, selectivity and “noise immunity” of DNA-sensors, using a polymer – CNT substrate and agents for the registration of hybridization

v) To develop measuring methods for the registration of the changes in biosensors properties stimulated by DNA hybridization or other processes.

A. Technical progress

A1. Team of the Yerevan State University

A1.1. Potential substrate preparation in collaboration with KiNSIS (Kiel University)

In order to construct a device based on DNA and/or RNA molecules, immobilized on conductive substrate, we have studied before the preparation of nanocomposite materials, including Polymers – CNT composites, functionalized and non – functionalized graphene nanoplatelets (GNPs) and their nanocomposites with polymers. To find a material that is most appropriate for our purposes we plan to investigate also zinc oxide (ZnO) is a unique material that exhibits semiconducting and piezoelectric dual properties. Using a solid–vapour phase thermal sublimation technique, nanocombs, nanorings, nanohelixes/nanosprings, nanobelts, nanowires and nanocages of ZnO have been synthesized under specific growth conditions.

To investigate the ZnO features we have contact with Prof. R. Adelung from the Kiel Nano, Surface and Interface Science (KiNSIS) Center (Kiel University, Germany). ZnO tetrapod sctructures ZnOT structures were synthesized by a recently developed flame transport synthesis (FTS) approach (Adelung et al., 2011). Briefly, the Zn metal micro powder (commercially available from Goodfellows, UK) was mixed with sacrificial polymer powder (Polyvinyl Butyrol, Kuraray GmbH Europe) and the mixture was then burned at 900 °C in a simple muffle type box furnace in air which resulted in the formation of ZnOTs (Adelung et al., 2011; Mecklenurg et al. (2012)).

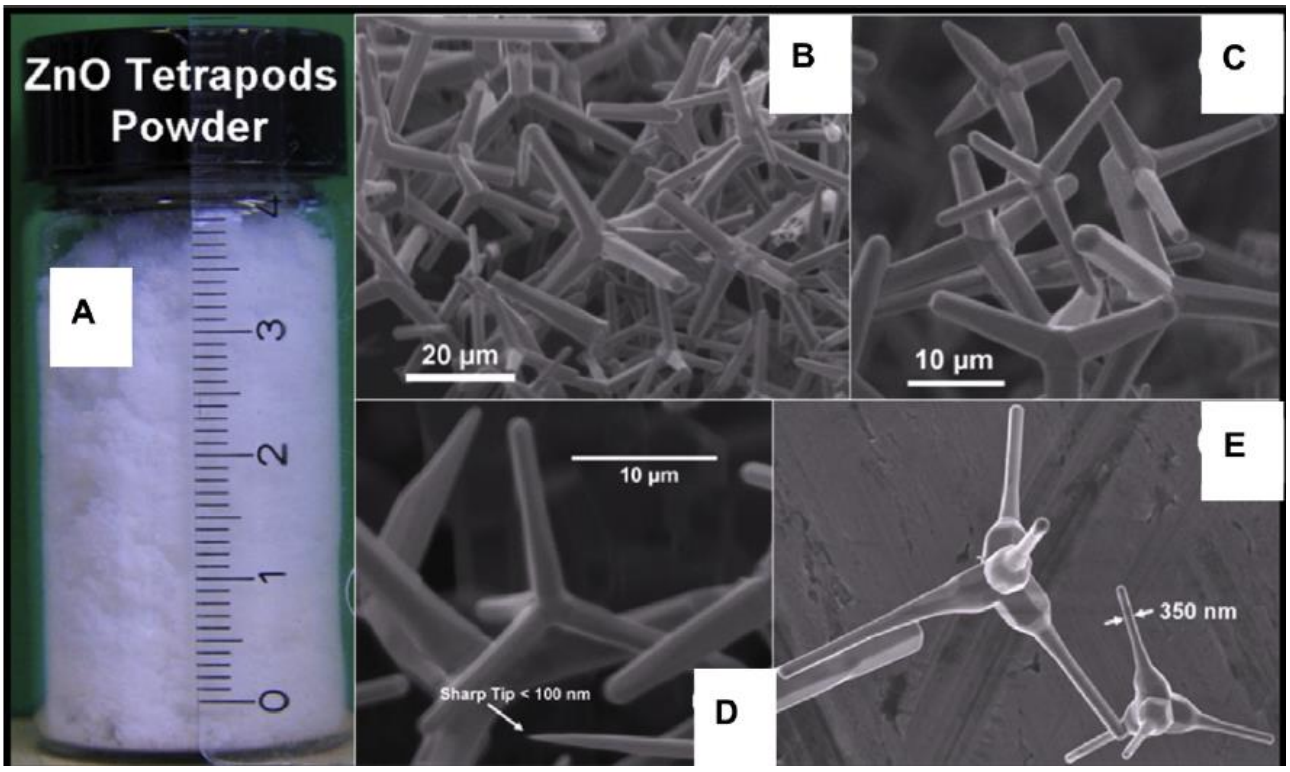

Fig. 1. *ZnO nano-micro scale tetrapod structures synthesized by flame transport approach: (A) Glass bottle shows the large amount of ZnO tetrapod structures which were synthesized in just one run. (B–E) show the scanning electron microscopy images of different type of tetrapod structures from the ZnO powder shown in (A).*

During Dr. Mamasakhlisov's visit (10 – 17 Aug, 2015) to the group of prof. R.Adelung (KiNSIS, Kiel University) the possible applications of the nanostructured ZnO for the DNA chips creation have been discussed and the possible directions of collaboration were discussed. From our side theoretical results, concerning DNA hybridization have been presented. The samples of tetrapod structured ZnO for the subsequent experiments in the groups of YSU and LNFN INFN were kindly provided by prof. R. Adelung and delivered to Armenia by Dr. Mamasakhlisov.

A1.2. Theoretical work, concerning ssDNA hybridization on the surface.

The results obtained below were presented at the International Symposium and Young Scientist School "Disordered and Ordered Materials Analysis and Characterization - DOM2015", 24-30 September 2015, Yerevan, Armenia

.

One of the important directions of DNA - chips improvement is the increasing selectivity and sensitivity in expense of enhancement of electric signal and target probe hybridization stability. Efficiency of such devices as DNA-sensors and DNA-chips depends on precise prediction of

experimental parameters responsible for thermostability of nucleic acids duplexes and specific times of formation of DNA duplexes [3]. Some following factors influence on the thermodynamics of hybridization, in particular: the density of single-strand DNA assays (the length 25-49 nucleotides) immobilized on the surface; the presence of competing hybridization; and some other factors.

Development of DNA-sensors imposes specific requirements on the effectiveness of hybridization on the interface solid-solution. One of the main requirements to the DNA-sensors is the high sensitivity and selectivity, which in its turn, demands a maximal effectiveness of hybridization and minimal non-specific adsorption on the interface of solid and liquid phases. The nucleic acids hybridization depends substantially on the temperature, salt concentration, viscosity, GC-content and other physical-chemical features. The increase of selectivity and sensitivity of DNA-sensors can be reached by using electro-chemically active compounds with higher affinity to the dsDNA than to the ssDNA. This kind of compounds can substantially increase the dsDNA stability and at the same time, the amplitude of generated signal, which increases the DNA-sensor sensitivity.

Among this kind of ligands are intercalators, molecules with flat heterocyclic structure, which fit between nucleic acids and change the local structure of dsDNA.

Below we are focused on the isotherm of hybridization of DNA on the surface in presence of ligands, binding with double - stranded regions of DNA. Let us compare the equilibrium hybridization isotherms for two idealized but experimentally accessible situations, where DNA chip immersed in solution containing intercalating ligands and: 1) only one type of single-stranded target or 2) containing targets of two different types that do not hybridize in the bulk but are both capable of hybridizing with the same probe on the surface.

The non-competitive hybridization

Let us consider the spot of N_0 single - stranded probes *p*, wherein the N_{pt} of them are hybridized with target *t*. The hybridization of *p* and *t* creates a double-stranded oligonucleotide, *pt*, at the surface. In simplest case of single species of ssDNA target, surface will be covered only by free probes *p* and hybridized ones *pt*. In this case the only reaction is

$$p + t \rightleftharpoons pt$$

and no competitive hybridization reactions occur.

$x = \frac{N_{pt}}{N_0}$ The dependence of the hybridization degree, , on the concentration of the target, c_t, is described by hybridization isotherm. For the intercalating ligands the binding reactions are written

$$
\begin{aligned}
pt + \ell &\rightleftharpoons pt_1 \\
pt_1 + \ell &\rightleftharpoons pt_2 \\
&\dots \\
pt_{N-1} + \ell &\rightleftharpoons pt_N,
\end{aligned}
$$

where *pt* is the free duplex, while pt_j is the target – probe duplex bound to *j* ligands *l* and *N* is the number of binding sites (number of nucleotides in simplified case).

In the mean field approximation the equilibrium state is defined by conditions

$$
\begin{aligned}
\mu_{pt} &= \mu_p + \mu_t \\
\mu_b &= \mu_\ell
\end{aligned}
$$

where μ_{pt} is the chemical potential of hybridized probe *pt*, μ_t is the chemical potential of target, μ_p is the chemical potential of probe, μ_b and μ_ℓ are the chemical potentials of the bound and free ligand, correspondingly. In the approximation of weak solution the chemical potential of the targets and ligands in the bulk the isotherm of hybridization is written

$$
\frac{x(1-r)^N}{c_t(1-x)} = K_t e^{-\frac{N}{k_B T}\frac{\partial \gamma_{el.}}{\partial \sigma}}
$$

where

and .

$$
K_t = e^{-\frac{\Delta G^0}{k_B T}}
$$

$$
\Delta G^0 = \mu^0_{pt} - \mu^0_p - \mu^0_t
$$

The equilibrium distribution of ligands (ℓ) between bound and free states is described by the isotherm of adsorption

$$
\frac{r}{c_\ell(1-r)} = K_\ell,
$$

c_ℓ where is concentration of ligands in the bulk, *r* is the degree of ligand adsorption and

$$K_\ell = e^{-\frac{\Delta g^0}{k_B T}} \text{ and } \Delta\, g^0 = \mu_b^0 - \mu_\ell^0.$$

The surface - competitive hybridization

Let us consider the second scenario, where solvent containing targets of two different types *t* and *m* that do not hybridize in the bulk but are both capable of hybridizing with the same probe *p* on the surface. *t* is the target sequence, complementary to the probe *p*, while *m* is the mismatched sequence only partially complementary to the probe *p*. It is supposed that the available number of binding sites for the intercalating ligands on the *pm* duplex is equal to *M* , where *M* < *N*.

If intercalation is the only mechanism of ligands binding, DNA-ligand complex formation will be restricted only by double-stranded regions. The chemical potential of the ligand bound to the complementary duplex pt is written

$$\mu_b^1 = \mu_b^0 + k_B T ln \frac{r_1}{1 - r_1},$$

where

$$r_1 = \frac{N_1}{N N_{pt}}$$

is the degree of ligand adsorption on the duplex *pt* , while the chemical potential of the ligand bound to the partially complementary duplex *pm* yields

$$\mu_b^2 = \mu_b^0 + k_B T ln \frac{r_2}{1 - r_2},$$

where

$$r_2 = \frac{N_2}{N N_{pm}}.$$

At the same time, the exchange chemical potentials for the hybridized probes *pt* and *pm* are written

$$\Delta\mu_{pt} = \Delta\mu^0_{pt} + k_B T \ln\frac{x}{1-x-y} + N k_B T \ln(1-r_1)$$
$$\Delta\mu_{pm} = \Delta\mu^0_{pm} + k_B T \ln\frac{y}{1-x-y} + N k_B T \ln(1-r_2),$$

where

$$y = \frac{N_{pm}}{N_0}.$$

The equilibrium between ligands, targets and mismatched sequences in solution and hybridized probes is satisfied by conditions

$$\mu^1_b = \mu_\ell$$
$$\mu^2_b = \mu_\ell$$
$$\Delta\mu_{pt} = \mu_t$$
$$\Delta\mu_{pm} = \mu_m,$$

The isotherms of hybridization obtained with in the framework of theory, proposed above are presented in the Fig. 2.

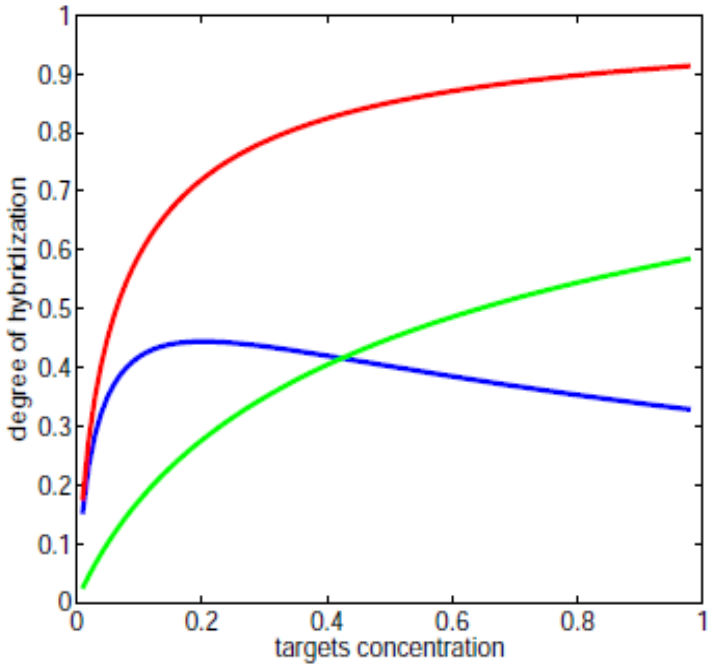

Fig. 2. *Isotherm of hybridization in: ligand-free case (green line); in presence of ligands (red line). The shift of the hybridization isotherm is indicated by blue line*.

Thus, intercalating ligands caused the substantially increases of the degree of hybridization. One of the important parameters, responsible for the DNA-chip sensitivity is the concentration of target

c_{50}^t leading to one-half equilibrium hybridization . The shift of the one – half concentration in comparison with ligand-free case yields

$$\delta c_{50}^t = \frac{e^{3\Gamma/2}}{K_t}\left[\left(\frac{K_\ell c_\ell}{1+K_\ell c_\ell}\right)^N - 1\right],$$

where

$$\Gamma = 8\pi N \sigma_0 \ell_B \frac{r_D^2}{H}$$

The one-half concentration shift depends on the concentration of ℓ ligands (see Fig. 3).

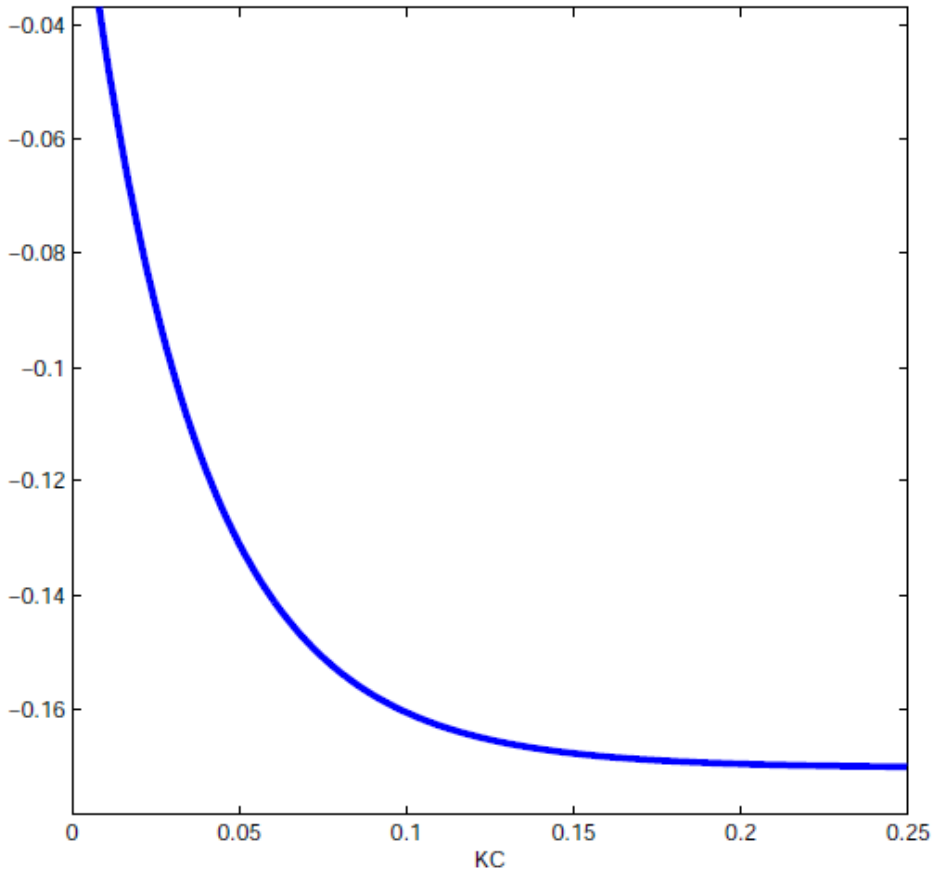

Fig. 3. *The shift of one-half concentration in dependence on* $K_\ell c_\ell$
.

Thus, the intercalating ligands binding with hybridized probes *pt* **substantially decreases the concentration of one – half hybridization and then affects the sensitivity of the DNA-chip in case of non-competitive hybridization**.

To address the effect of ligand binding on the selectivity of DNA – chip we compare the complementary hybridization degree with the partial one and obtained

$$\frac{x}{y} = \frac{c_t}{c_m}\frac{K_t}{K_m}e^{-(N-M)\ln(1-r^*)}$$

where

$$r^* = \frac{c_\ell K_\ell}{c_\ell K_\ell + 1}$$

is the equilibrium value of the degree of adsorption. **Thus, the effect of the ligands is more pronounced for the target sequences *t* because of exponential dependence on the parameter *(N-M)*. If the number of binding sites *M* for the mismatched duplex *pm* differs significantly from those for the complementary duplex *pt (N)*, we can obtain the substantial increases of selectivity.**

A1.3. Theoretical work, concerning ssRNA folding and hybridization (see the previous reports for details)

Paper is published: **Collapse and hybridization of RNA: view from replica technique approach**, Y. Sh. Mamasakhlisov, S. Bellucci, Sh. Hayryan, H. Caturyan, Z. Grigoryan, and C.-K. Hu, Europhys. J. E **38**, 100(1-9) (2015)

DOI 10.1140/epje/i2015-15100-x.

A1.4. Theoretical work, concerning solvent effects in the stability of the DNA duplex

The results obtained below are published in: **Solvent effects in the helix-coil transition model can explain the unusual biophysics of intrinsically disordered proteins**

, A. Badasyan, Y. Sh. Mamasakhlisov, R. Podgornik, and V. A. Parsegian

, J. Chem. Phys. **143**, 014102(1-7) (2015).

We analyze a model statistical description of the helix-coil transition in terms of Potts – like model, where we
take into account the specificity of its primary sequence, as quantified by the phase space volume ratio of the number of all accessible states to the number corresponding to a helical conformation. Phase diagrams are obtained in terms of the temperature – pressure variables

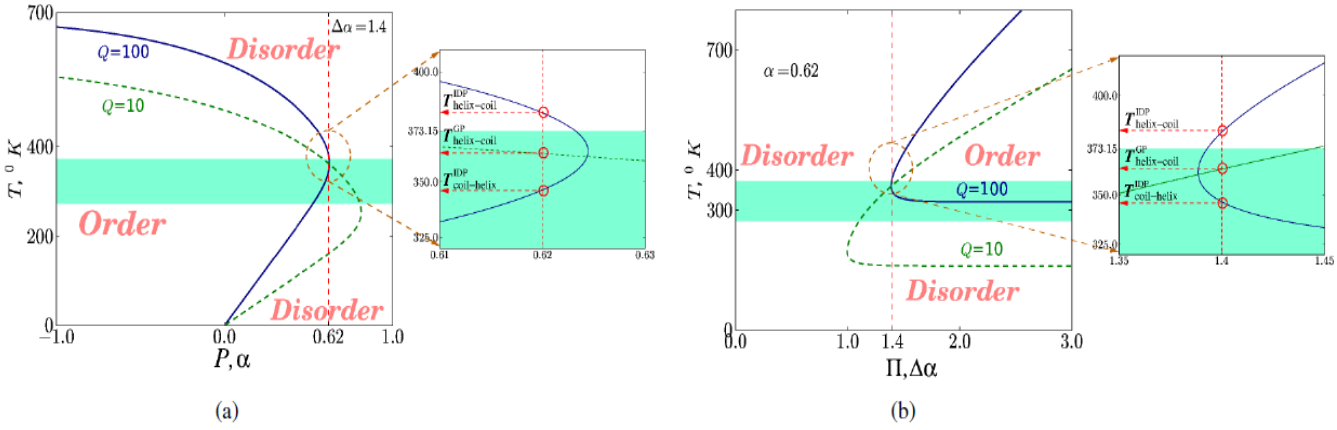

Fig. 4. *Phase diagrams obtained numericlly on the basis of the Potts – like model. Temperature is in degrees Kelvin, pressure in dimensionless units of α, and osmotic stress in dimensionless units of Δα. The following set of parameters is used: Δ = 3, q = 10, p = 100. Insets show the presence of the helix-coil transition (Q= 10) and coil-helix or cold denaturation (Q= 100) within the range of physiological temperatures. Outside of this physiological range, above the water boiling point, is the helix-coil transition , and below the water freezing point, the cold denaturation (not shown). The projection of phase diagram (a) in the pressure-temperature plane is plotted at Δα = 1.4,p and (b) in the osmotic stress-temperature plane is plotted at α = 0.62.*

Here, **we argue how the nature of this modified phase diagram, obtained from a model of the helix-coil transition in a solvent, would illuminate the turned-out response of macromolecules such as nucleic acids and proteins, to the changes in the environment conditions that follow straightforwardly from the re-entrant (cold denaturation) branch in their phase diagram**.

A1.5. Project publications:

1. **Collapse and hybridization of RNA: view from replica technique approach**, Y. Sh. Mamasakhlisov, S. Bellucci, Sh. Hayryan, H. Caturyan, Z. Grigoryan, and C.-K. Hu

, Europhys. J. E **38**, 100(1-9) (2015)

DOI 10.1140/epje/i2015-15100-x.

2. **Solvent effects in the helix-coil transition model can explain the unusual biophysics of intrinsically disordered proteins**

, A. Badasyan, Y. Sh. Mamasakhlisov, R. Podgornik, and V. A. Parsegian

, J. Chem. Phys. **143**, 014102(1-7) (2015).

3. **Hybridization isotherm of DNA chip: the effect of ligand binding,** Sh. Tonoyan, V. Morozov, Y. Mamasakhlisov, Book of Abstracts, International Symposium and Young Scientist School "Disordered and Ordered Materials Analysis and Characterization - DOM2015", 24-30 September 2015, Yerevan, Armenia.

A2. Team of the LNF, INFN

A2.1 Functionalization of GNPs with porphyrin.

The functionalization carried out in the second report are implemented by GNP functionalization with Prato's reaction in collaboration with Prof. P. Tagliatesta (University of Roma Tor Vergata).

We use an aldehydic substrate containing both a porphyrin and a ferrocene, linked by a triple bond each one.

The reaction develop as scheme reaction reported below

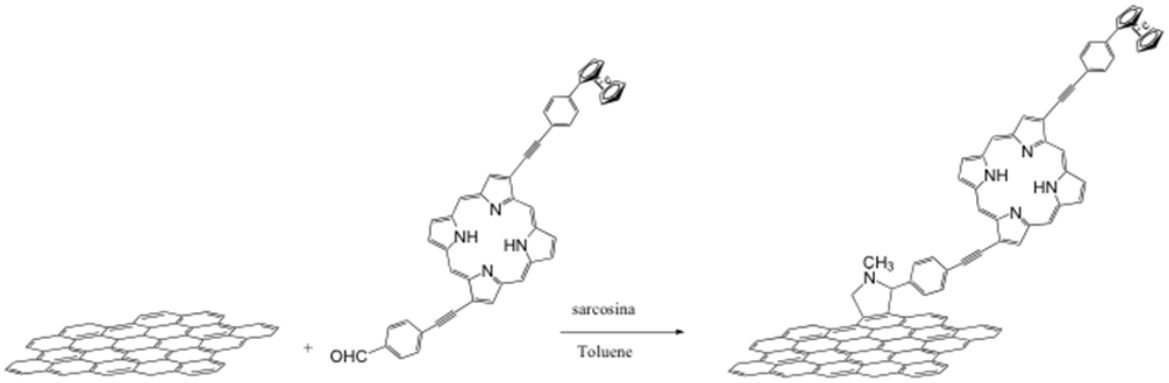

Scheme 1 Prato's reaction on GNP as substrate

After reaction, we observe functionalized GNP by SEM to check transformation on morphology of substrate.

The following figures represent a sample of pristine GNP:

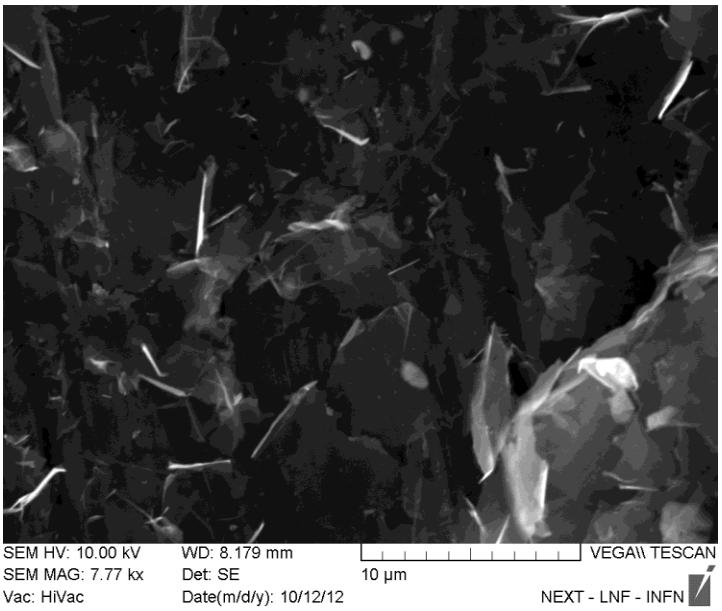

Figure 1 Micrograph of pristine GNP

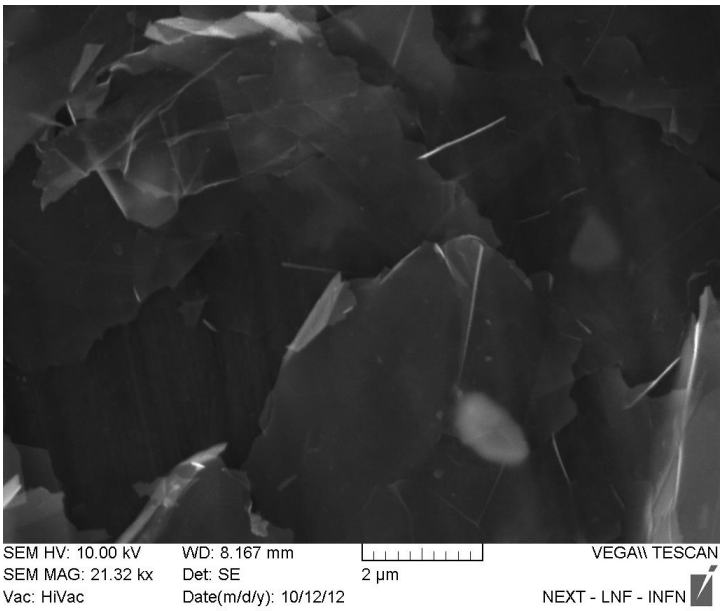

Figure 2 Micrograph of pristine GNP

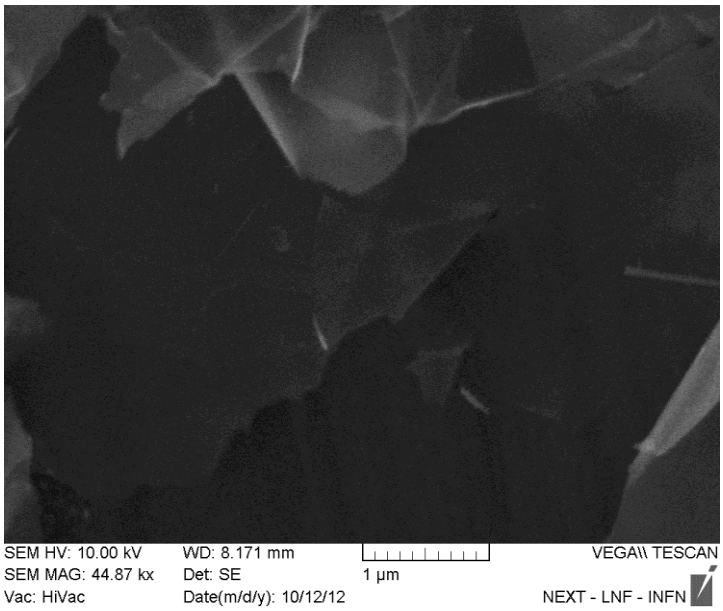

Figure 3 Micrograph of pristine GNP

We observe from micrographs that particles have average dimension of 5µm, separated each one.

The following figures represent a sample of functionalized GNP:

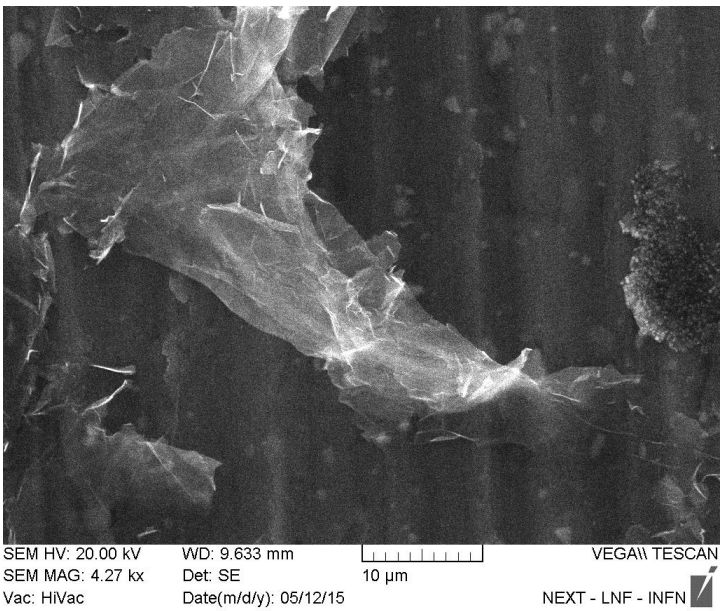

Figure 4 Micrograph of functionalized GNP

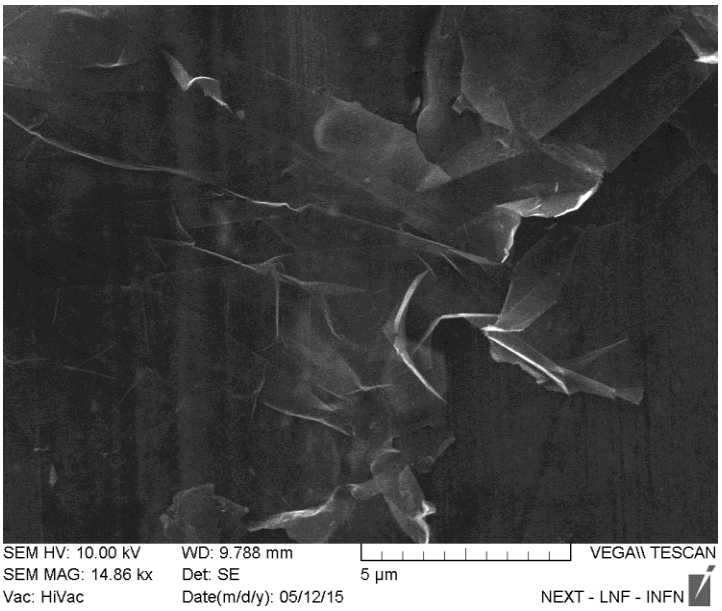

Figure 5 Micrograph of functionalized GNP

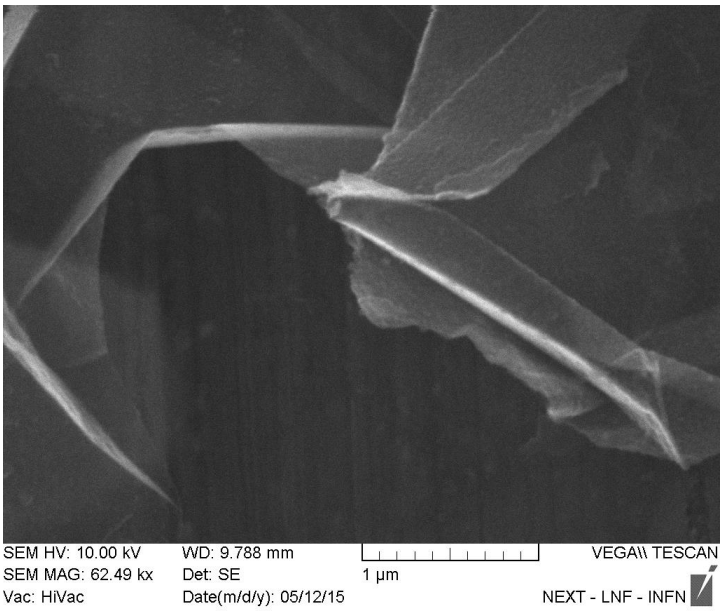

Figure 6 Micrograph of functionalized GNP

We observe from micrographs that particles are cohesive instead of pristine particles.

To confirm the functionalization, we characterized the material with Raman spectroscopy in collaboration with Dr. V. Mussi (CNR-ISC).

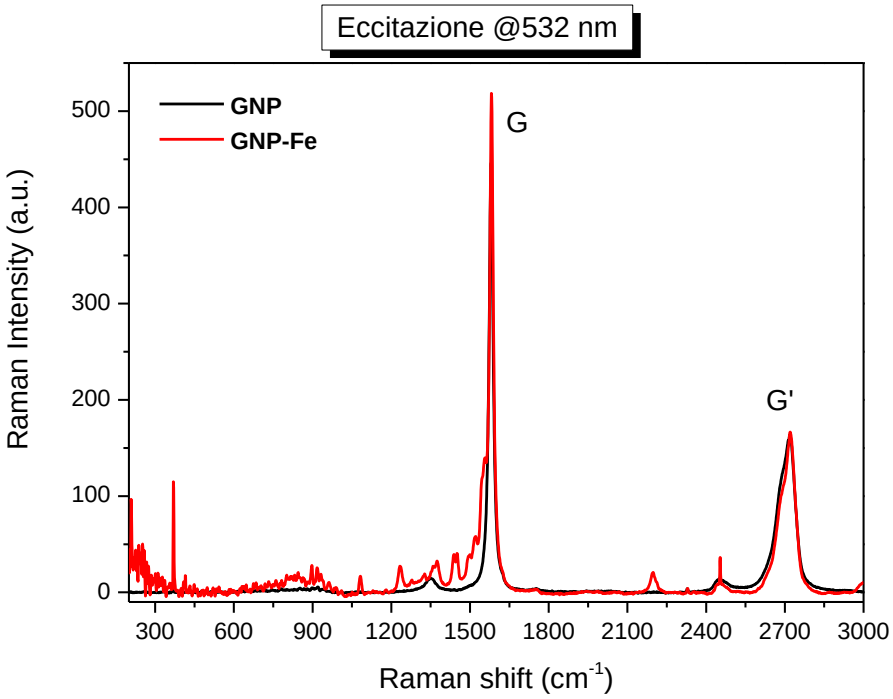

Figure 7 Raman spectrum of pristine and functionalized GNP

The comparison between the spectra of pristine and functionalized GNP reveals that functionalization occurs. Indeed, new peaks appear in the spectrum of functionalized GNP, attributable to presence of porphyrin/ferrocene. Enlarge spectra are reported below:

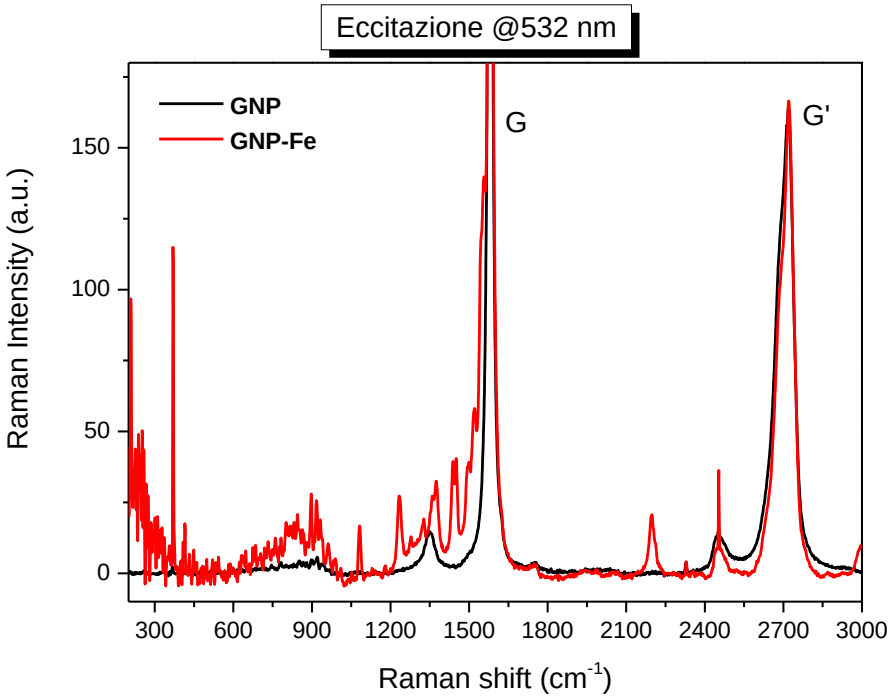

Figure 8 Raman spectrum of pristine and functionalized GNP zoom in

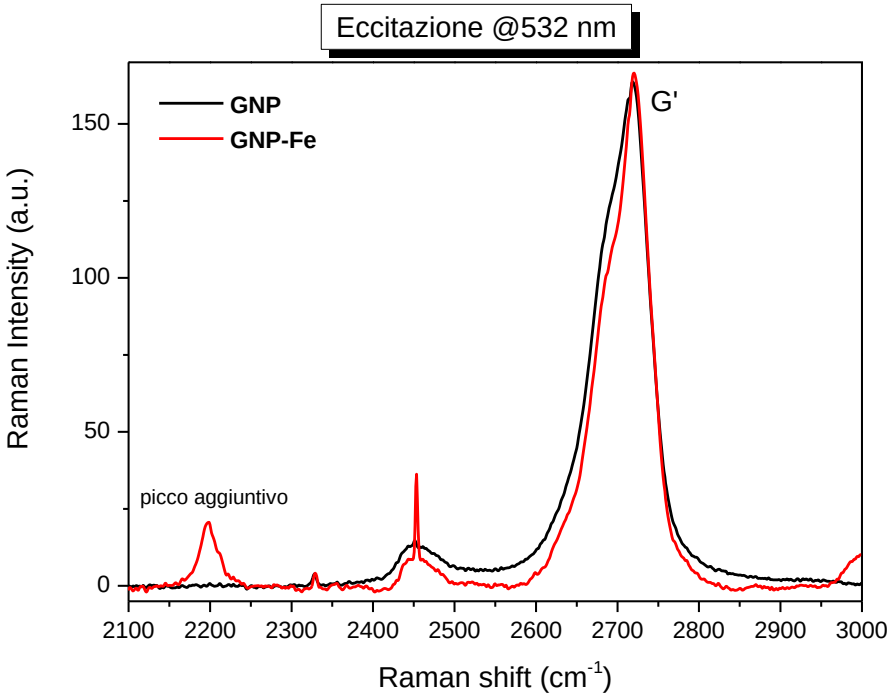

Figure 9 Raman spectrum of pristine and functionalized GNP zoom in

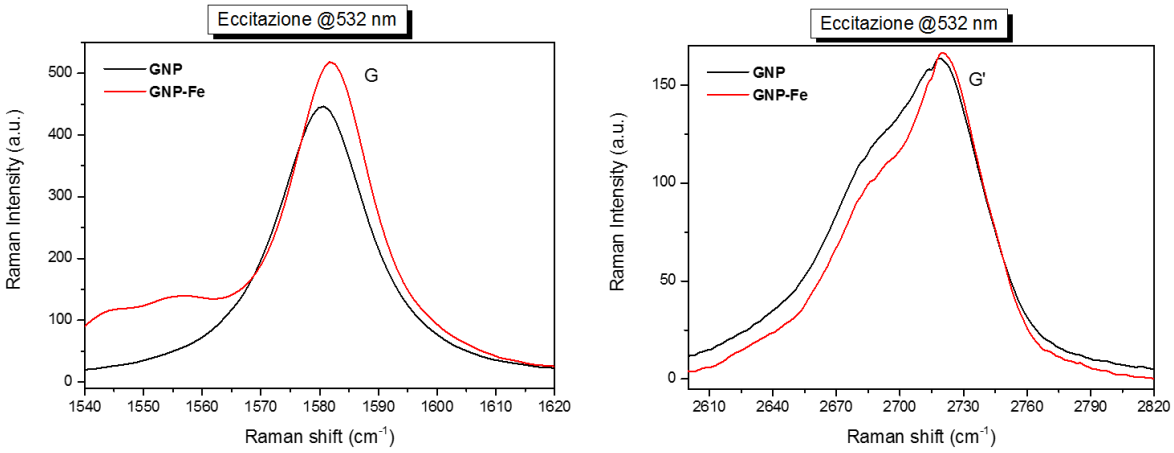

Figure 10 Raman spectrum of functionalized GNP zoom in

The shift of G and G' band of graphene at higher wavenumber confirms that functionalization occurs.

A2.2 Preparation of free-standing paper of GNP to used as platform for biosensor.

We explore a new platform to host the biosensor. We think to compare the electrochemical properties of filler inside and outside epoxy resin.

Nowadays, freestanding paper of CNT are commercial available. For GNP, freestanding paper has not yet available.

We carried out an experiment to prepare freestanding of GNP.

A dispersion of GNP in water was prepared and sonicated with an ultrasonic tip for two minute. Then, dispersion has filtrated with an alumina filter. The filter was put under a weight of 10kg for 5min. The paper of GNP was removed with a scalpel from the filter and dried in oven at 80°C overnight. Images of the paper made of graphene are reported below:

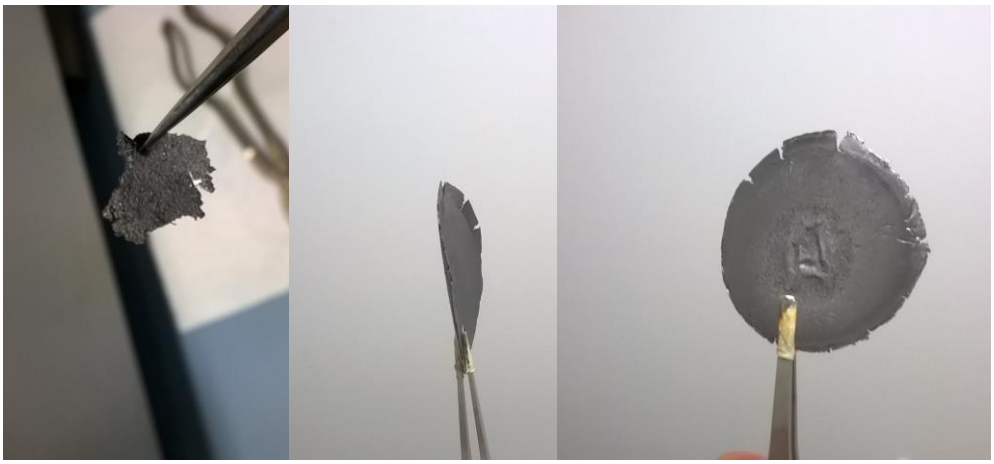

Figure 11 Picture of paper of GNP

We characterize paper of GNP by SEM, reported in the following pictures:

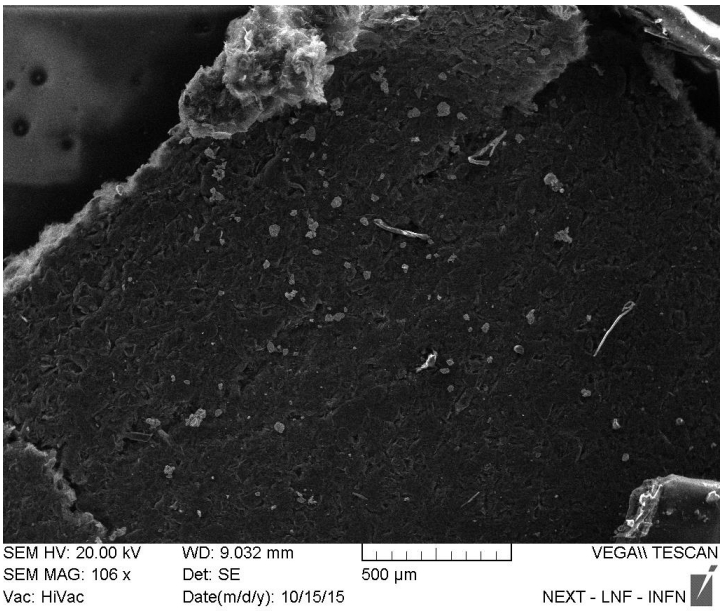

Figure 12 Micrograph of paper of GNP

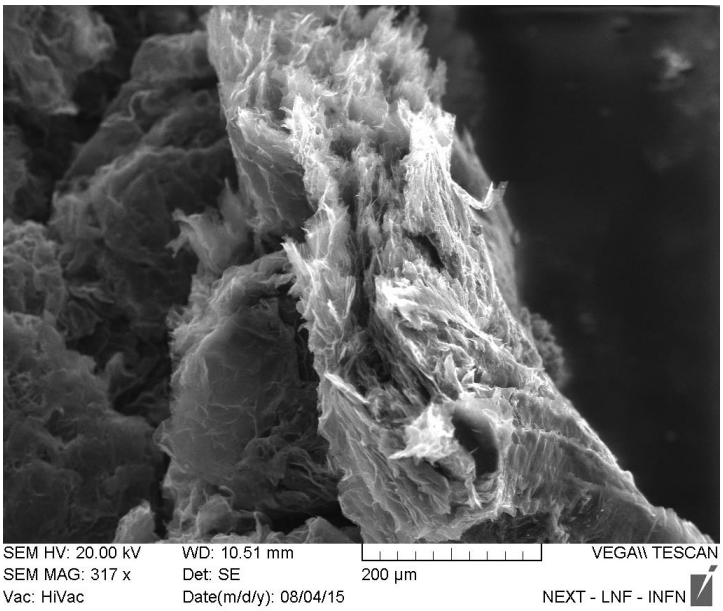

Figure 13 Micrograph of paper of GNP

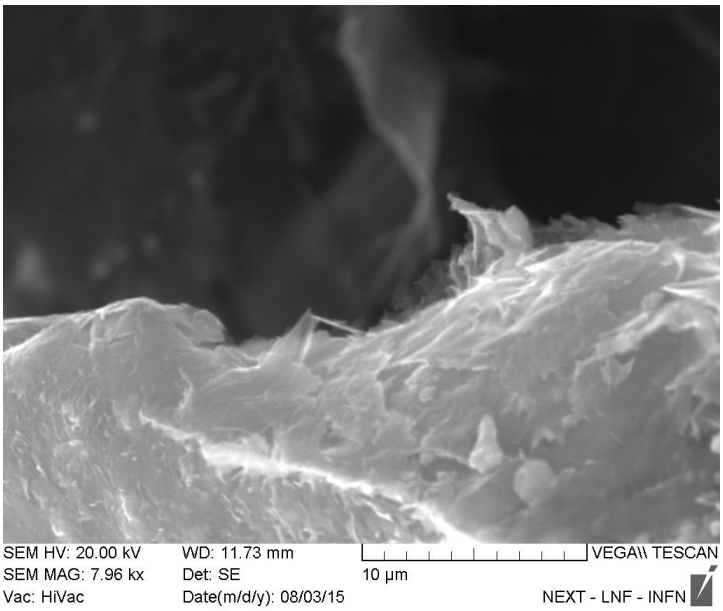

Figure 14 Micrograph of paper of GNP

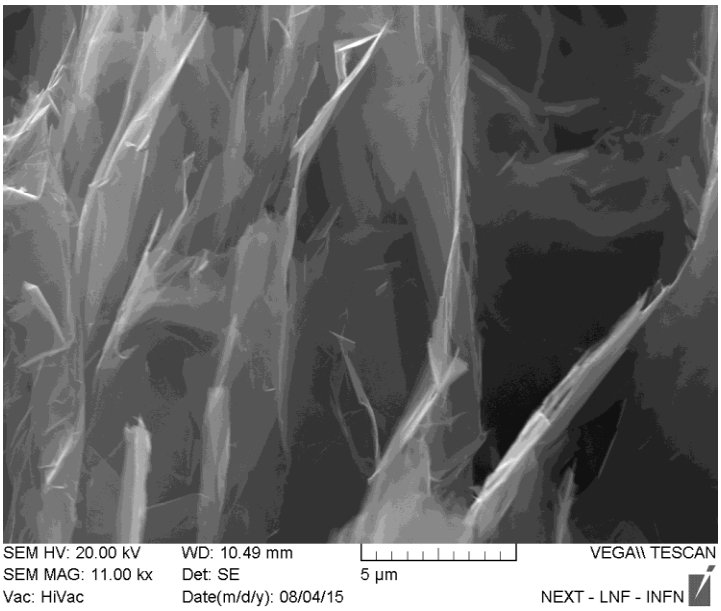

Figure 15 Micrograph of paper of GNP

Paper of GNP has a fine texture and a compact surface. Nevertheless, GNP maintain proper thickness, as revealed from lateral images.

A2.3 Electrochemical analysis

We have investigated the electrochemical behavior of pure epoxy resin and epoxy resin loaded with CNT and GNP.

This study has been performed EIS and CV characterization by using PalmSens^3 instrument.

Pure Epoxy resin

The first step consists in studying the electrochemical behavior of pure epoxy resin performing a CV. We have chosen as experimental setup: a solution 1 mM of $K_3[Fe(CN)_6]$, a voltage range of -0.1/0.6 V, 100 mV/s scan rate, Ag/AgCl as reference electrode. As we can see in the following graphic, the redox process for the species Fe^{2+}/Fe^{3+} in solution does not occur at the resin interface.

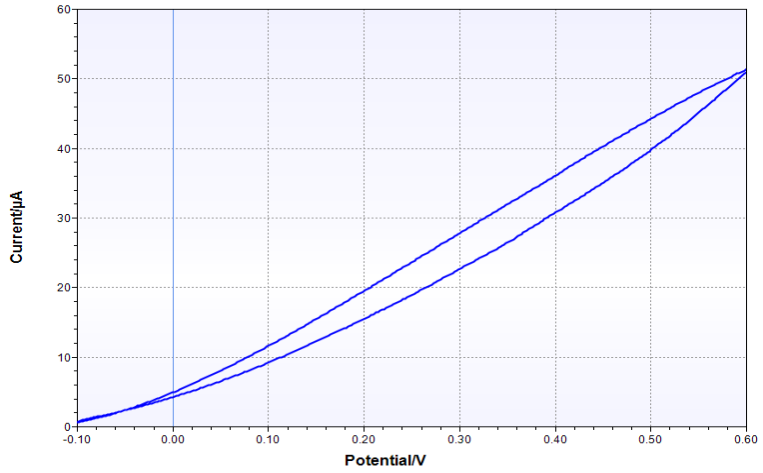

Figure 16 CV epoxy resin

It is possible to go deep about epoxy-resin interface behavior performing an EIS in the same solution mentioned before. We have scanned the frequencies range 10000/5 Hz. Nyquist plot confirms the CV result. This is a preliminary and qualitative study, we are working to find a fitting circuit to evaluate the R_{CT}.

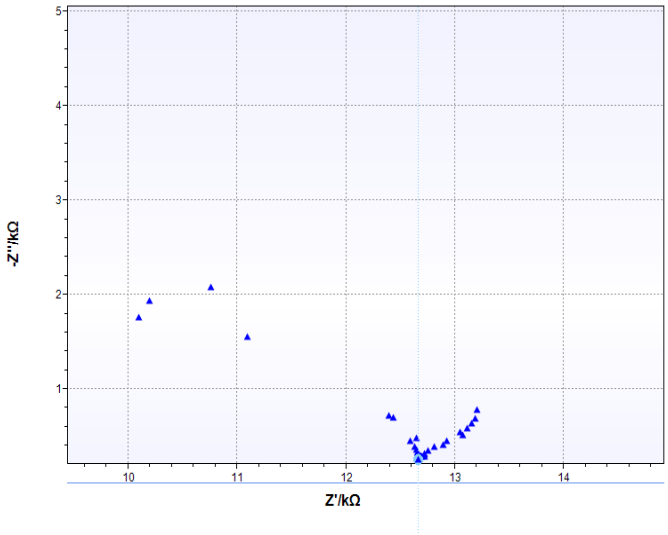

Figure 17 Nyquist plot epoxy resin

GNP composite

We tried to improve the epoxy resin electrochemical behavior by adding GNP realizing a nanocomposite. We have used the same experimental setup to performing CV characterization. We found performing a CV is that the electrochemical properties do not improve at all.

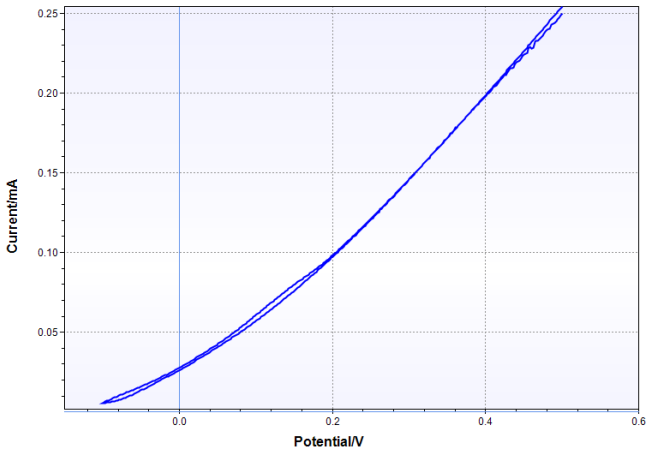

Figure 18 CV GNP nanocomposite 0.75%$_{w/w}$

Nevertheless, the EIS performance shows a reduced R_{CT}, as we can see in the figure 18, which suggests us an increasing of electrical properties compared with pure epoxy resin. We are working to find a fitting circuit to evaluate the R_{CT}.

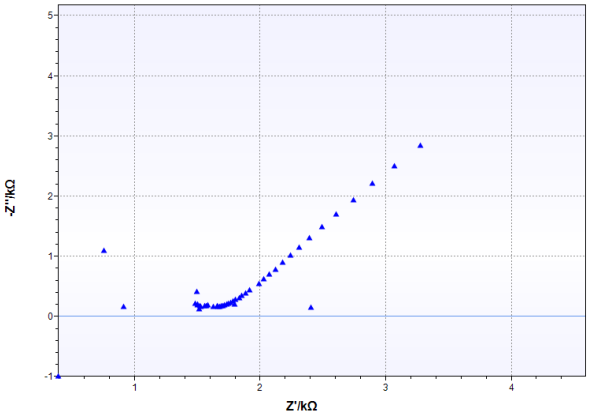

Figure 19 Nyqist plot GNP composite 0.75%$_{w/w}$

The next investigation will be performed by adding CNTs to resin and investigate how they improve electrochemical composite behavior. Furthermore, we will investigate any functionalization of nanocomposite surface to improve electrochemical properties.

A2.4 Preparation of nanocomposite materials with Thinky planetary mixer

Finally, we reported preliminary experiments carried out with Thinky planetary mixer, installed 12th October.

We want improuve the homogeneity of nanocomposite reducing the presence of bubble gas inside the matrix. For these reasons, we have worked in vacuum (3mbar) and changed mixing velocity. To test the new instrument at critical condition, we have prepared a nanocomposite loaded with 10%$_{w/w}$ of MWCNT 30-50 nm.

After preparation, nanocomposite appears uniform and without bubble, as shown by picture reported below

Figure 20 Nanocomposite Epoxy/CNT 10% $_{w/w}$

We characterized sample with SEM and we observed the two side: the one attached to beaker and the one to the air.

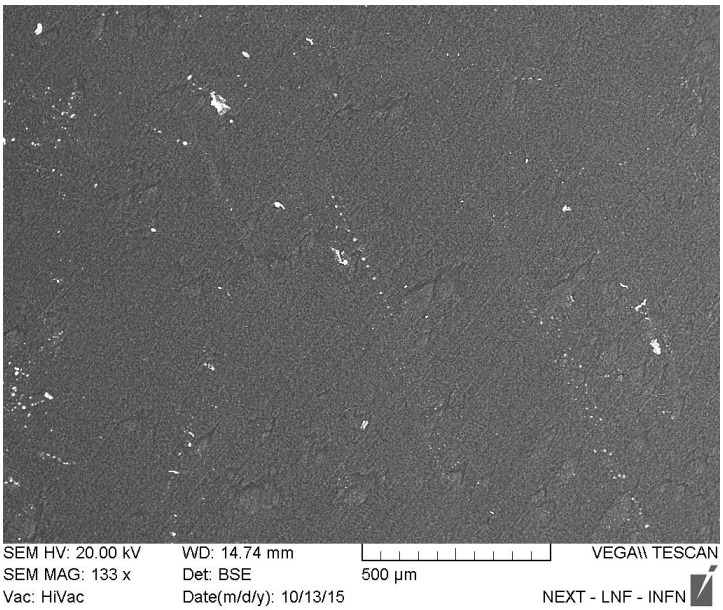

Figure 21 Micrograph of Nanocomposite Epoxy/CNT 10% $_{w/w}$ on air side

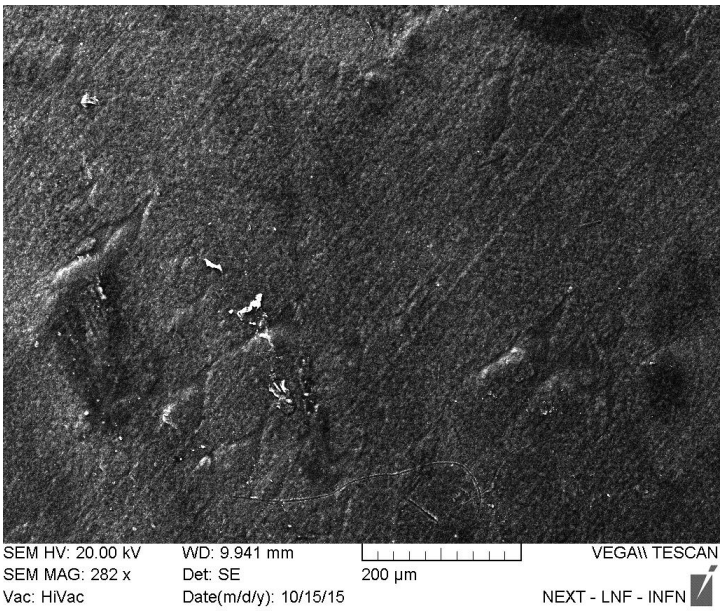

Figure 22 Micrograph of Nanocomposite Epoxy/CNT 10% $_{w/w}$ on air side

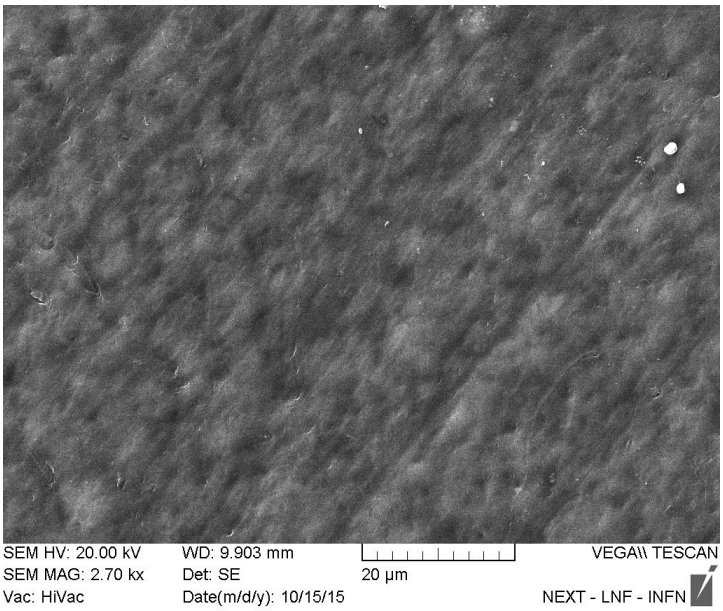

Figure 23 Micrograph of Nanocomposite Epoxy/CNT 10% $_{w/w}$ on air side

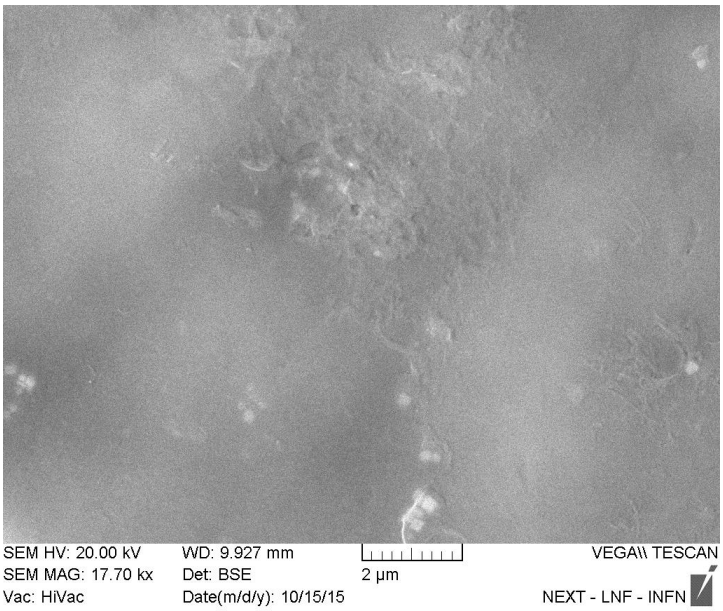

Figure 24 Micrograph of Nanocomposite Epoxy/CNT 10% $_{w/w}$ on air side

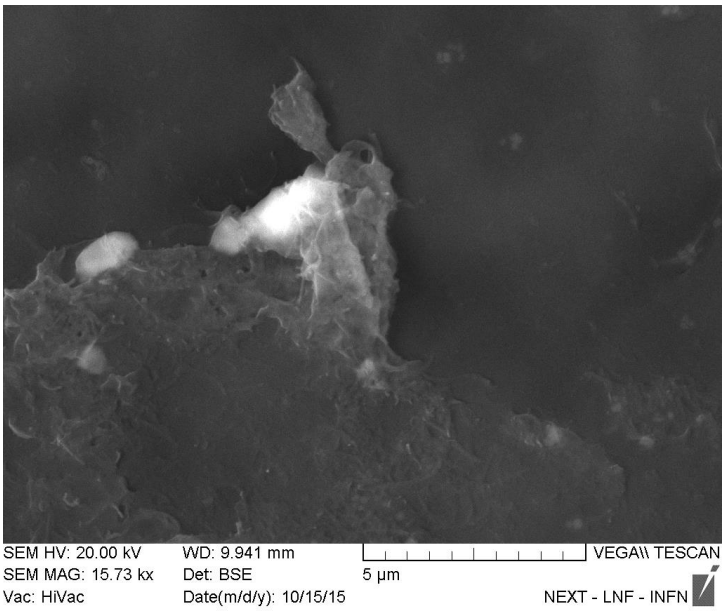

Figure 25 Micrograph of Nanocomposite Epoxy/CNT 10% $_{w/w}$ on air side

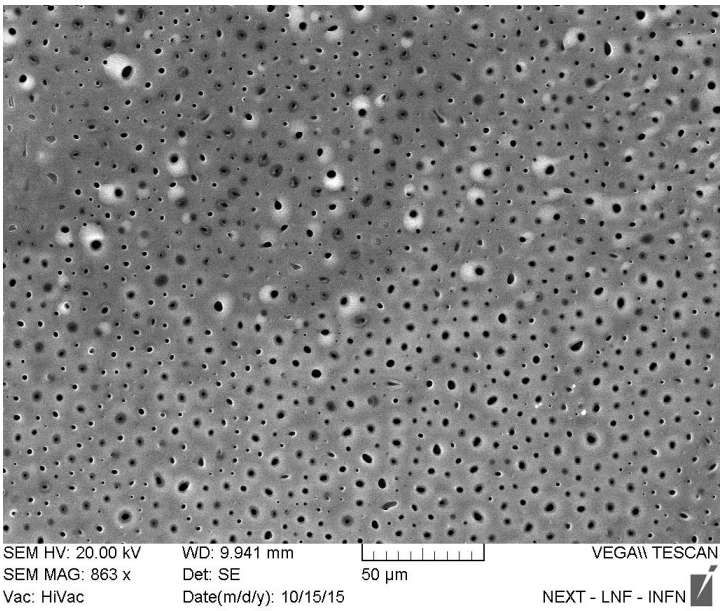

Figure 26Micrograph of Nanocomposite Epoxy/CNT 10% $_{w/w}$ on beaker side

We can see from picture that:

- matrix has not bubbles of air inside;

- MWCNT are well dispersed in matrix, although some aggregates;

- matrix from beaker side copy the structure of beaker.

In conclusion, first results are promising to improve homogeneity of nanocomposites.

A2.1. Project publications:

1. **Collapse and hybridization of RNA: view from replica technique approach**, Y. Sh. Mamasakhlisov, S. Bellucci, Sh. Hayryan, H. Caturyan, Z. Grigoryan, and C.-K. Hu,

The European Physical Journal E **38**, 1-9 (2015)

2. **What does See the Impulse Acoustic Microscopy inside Nanocomposites?**

VM Levin, YS Petronyuk, ES Morokov, A Celzard, S Bellucci, PP Kuzhir, Physics Procedia **70,** 703-706 (2015).

3. **Electromagnetic characterization of graphene and graphene nanoribbons via ab-initio permittivity simulations,** S Bellucci, A Sindona, D Mencarelli, L Pierantoni, 2015 International Conference on Electromagnetics in Advanced Applications (ICEAA), 926-929, Editor IEEE.

4. **Synthesis and electrical characterization of Graphene Nanoplatelets,** A Maffucci, F Micciulla, A Cataldo, G Miano, S Bellucci, 2015 International Conference on Electromagnetics in Advanced Applications (ICEAA), 301-304, Editor IEEE.

5. **Applications of Graphene at Microwave Frequencies,** M. Bozzi, L Pierantoni, S Bellucci, Radioengineering **24** (3), 661 (2015).

6. **Broadband Microwave Attenuator Based on Few Layer Graphene Flakes,** L Pierantoni, D Mencarelli, M Bozzi, R Moro, S Moscato, L Perregrini, F. Micciulla, A. Cataldo, S. Bellucci, IEEE Transactions on Microwave Theory and Techniques, Aug. 2015, vol. **63**, no. 8, p. 2491–2497. DOI:

10.1109/TMTT.2015.2441062.

7. **Spatial dispersion effects upon local excitation of extrinsic plasmons in a graphene micro-disk,** D Mencarelli, S Bellucci, A Sindona, L Pierantoni, arXiv preprint arXiv:1507.07090661 Journal of Physics D: Applied Physics (2015).

8. **On the absence of actual plateaus in zero-temperature magnetization curves of quantum spin clusters and chains,** V Ohanyan, O Rojas, J Strecka, S Bellucci, Physical Review **B 92** (21), 214423, arXiv preprint arXiv:1506.02933 (2015).

9. **Microstructure, elastic and electromagnetic properties of epoxy-graphite composites,** S Bellucci, F Micciulla, VM Levin, YS Petronyuk, LA Chernozatonskii, PP Kuzhir, AG Paddubskaya, J Macutkevic, MA Pletnev, V Fierro, A Celzard, AIP Advances **5** (6), 067137 (2015).

10. **Multiwalled carbon nanotube buckypaper induces cell cycle arrest and apoptosis in human leukemia cell lines through modulation of AKT and MAPK signaling pathways,** S Dinicola, MG Masiello, S Proietti, P Coluccia, G Fabrizi, A Palombo, F. Micciulla, S. Bistarelli, G. Ricci, A. Catizone, G. De Toma, M. Bizzarri, S. Bellucci, A. Cucina, Toxicology in Vitro **29,** 1298–1308 (2015).

11. **Growth inhibition, cell-cycle alteration and apoptosis in stimulated human peripheral blood lymphocytes by multiwalled carbon nanotube buckypaper,** O Zeni, A Sannino, S Romeo, F Micciulla, S Bellucci, MR Scarfi, Nanomedicine **10** (3), 351-360 (2015).

12. **Sharp variations in the electronic properties of graphene deposited on the h-BN layer,** DG Kvashnin, S Bellucci, LA Chernozatonskii, Physical Chemistry Chemical Physics **17** (6), 4354-4359 (2015).

13. **Biological interactions of carbon-based nanomaterials: From coronation to degradation**, K Bhattacharya, SP Mukherjee, A Gallud, SC Burkert, S Bistarelli, S. Bellucci, M. Bottini, A. Star, B. Fadeel, Nanomedicine: Nanotechnology, Biology and Medicine, Volume **12**, Issue 2, February 2016, Pages 333–351

List of Conference Talks by LNF Authors in the Year 2015

S. Bellucci, Carbon nanostructures in biology and medicine, Nanomeeting 2015, Minsk (Belarus), 26-29 May 2015

S. Bellucci, What Next in Condensed Matter, INFN-LNF, Frascati (Italy), Feb 27, 2015.

S. Bellucci, Research Seminar, Unical Cosenza (Italy), 10 March 2015

S. Bellucci, Engineered Nanomaterials Health Effects, Nanoscience and Nanotechnology 2015, INFN-LNF Frascati (Italy), 28 september - 02 October 2015.